

Heterobi-, tri- and tetra-metallic cyanide-bridged complexes based on pentacarbonylcyanochromate(0) and penta-, *cis*-tetra- and *fac*-tri-ammineruthenium(III) groups: optical metal–metal charge transfer and electrochemical characteristics

W.M. Laidlaw, R.G. Denning*

Inorganic Chemistry Laboratory, South Parks Road, Oxford OX1 3QR, UK

Received 15 August 1995; revised 26 October 1995

Abstract

The heterobi-, tri- and tetra-metallic Robin-Day Class II mixed-valence complexes, $[(OC)_5Cr(\mu-CN)Ru(NH_3)_5]^{2+}$ (**CrRu**), *cis*- $[(OC)_5Cr(\mu-CN)_2Ru(NH_3)_4]^+$ (**Cr₂Ru**) and *fac*- $[(OC)_5Cr(\mu-CN)_3Ru(NH_3)_3]$ (**Cr₃Ru**) have been synthesised directly by coupling $[Cr(CO)_5CN]^-$ with an appropriate penta-, tetra- or tri-ammineruthenium precursor and characterised by electrochemical, analytical and spectroscopic methods. The complexes exhibit solvent–ammine hydrogen-bonding induced solvatochromism in the MMCT energy which linearly varies with the Gutmann solvent donor number (DN) at 219, 158 and $116(\pm 7)$ cm^{-1}/DN respectively which corresponds to a linear variation of $51(\pm 6)$ $cm^{-1}/DN/NH_3$ group. Electrochemical and spectroscopic evidence points to the ligating equivalence of $[Cr(CO)_5CN]^-$ and NH_3 groups in this series. Cyclic and square-wave voltammograms, CV and SWV, show reversible couples at +0.45 and –0.36 V (versus ferrocene) for the chromium(0/I) and ruthenium(III/II) potentials in the complex set. Dispersion in CV and peak broadening in SWV, for **Cr_xRu** ($x=2, 3$), indicate weak Cr–Cr coupling through the ammineruthenium centre corresponding to a separation of ~65 mV. We report electrochemical data for $[(OC)_5Cr(\mu-CN)Os(NH_3)_5]^{2+}$ (**CrOs**) and its visibly spectacular solvatochromism (188 cm^{-1}/DN) from blue to purple, red, orange and yellow colourations.

Keywords: Metal–metal charge transfer; Chromium complexes; Ruthenium complexes; Cyanide complexes; Polymetallic complexes

1. Introduction

The cyanide-bridged low-spin d^6 – d^5 bimetallic fragment, $X(\mu-CN)Y$, is the basic unit of a large number of literature reports [1–3] centred around the study of various electronic phenomena associated with the optical metal(X)-to-metal(Y) (or intervalence) charge transfer (MMCT) absorption. Part of the attraction of this simple system is that the cyanide bridge can stabilise, through its π -acidic C-centred and σ -basic N-centred frontier orbitals, metals of significantly different electronic potential whilst simultaneously providing a short enough bridge, maintaining intermetallic coupling, to observe MMCT. For such systems the t_{2g} orbital hole is only slightly delocalised (< 5%) across the two metal sites and is described using the Robin–Day [4] Class II mixed-valence formalism.

Only recently have some trimetallic analogues [5–14] of the form, $X(\mu-CN)Y(\mu-NC)Z$, been reported as natural

extensions to the array of known bimetallic systems. For example, amongst a limited number of publications, Vogler and co-workers [10,11] have studied photochemical redox processes in, $[(NH_3)_5Co^{III}(\mu-NC)Co^{III}(CN)_4(\mu-CN)Ru^{II}(CN)_5]^{3-}$. Scandola and co-workers [5–7] have probed photophysical properties associated with *cis*- $[Ru(bpy)_2(CN)_2]$ N-bound to various metal fragments whereas Bocarsly and co-workers [12,13] have considered multielectron charge transfer in *trans*- $[(CN)_5Fe^{II}(\mu-CN)Pt^{IV}(NH_3)_4(\mu-NC)Fe^{II}(CN)_5]^{4-}$.

Part of our interest [2,3,15–17] has been to use and study first and second coordination sphere effects to perturb the electronic potential of one metal centre in a bimetallic unit to modify and tune the MMCT energy and associated electronic and optical properties. In this paper we supplement some of our existing bimetallic work [2,3] and extend it to tri- and tetra-metallic species based on one-, two- and three-metal donor fragments, $[Cr(CO)_5CN]^-$, coordinated to a single polyammineruthenium acceptor group. The complexes dis-

* Corresponding author.

cussed presently are, $[(OC)_5Cr(\mu-CN)Os(NH_3)_5]^{2+}$, $[(OC)_5Cr(\mu-CN)Ru(NH_3)_5]^{2+}$, *cis*- $[(OC)_5Cr(\mu-CN)_2Ru(NH_3)_4]^+$ and *fac*- $[(OC)_5Cr(\mu-CN)_3Ru(NH_3)_3]$ which we henceforth abbreviate to **CrOs**, **CrRu**, **Cr₂Ru** and **Cr₃Ru**, respectively.

2. Experimental

2.1. Physical measurements

IR spectra were recorded using pressed KBr pellets on a Mattson Polaris FTIR instrument. Electronic absorption spectra were obtained using Shimadzu UV–VIS–NIR (model UV-365), Perkin-Elmer (model 330) and Perkin-Elmer (model 552) spectrometers using 1 cm pathlength cuvettes with pure solvent as a reference sample. The following solvents were used as received: from Aldrich, acetone (HPLC, 99.9+%), acetonitrile (HPLC, 99.9+%), dimethylformamide (HPLC, 99.9+%) and chloroacetonitrile (99%); from Fluka, dimethylsulfoxide (puriss, absolute, 99.5%) and hexamethylphosphoramide (~97%); from Lancaster, nitromethane (~99.5%, GC; by personal communication). Trimethylphosphate (99%, GC, Aldrich) was passed through a column (1 × 7 cm) of neutral dry alumina (prepared by heating alumina at ~300 °C over ~3 h under vacuum and cooling in a dry atmosphere prior to use). Electrochemical measurements were undertaken using an Eco-Chemie Autolab potentiostat (PGSTAT20) running under GPES3 computer software. Cyclic voltammograms (CV) were recorded with scan rates from 20–500 mV s⁻¹. Standard square-wave [18] voltammograms (SWV) were obtained using a pulse amplitude (E_{sw}) of 50 mV, at a frequency of 25 Hz with a stepping potential (E_{st}) of 5 or 10 mV. Voltammograms were recorded, under argon, with and without the addition of the internal standard ferrocene. The reference electrode was a saturated KCl(aq) calomel separated from the sample compartment via a lugin capillary. The working electrode was a planar glassy carbon disc (diameter ~5 mm) which was wiped clean after each measurement. The counter electrode consisted of a Pt wire mesh. The conducting solutions were 0.1 M tetrabutylammonium tetrafluoroborate in acetonitrile (HPLC). Integration of square-wave difference current peaks were performed using a macro in Kaleidagraph™ software on a Macintosh computer. Microanalyses (C, H, N) were undertaken by the departmental facility. Chromium and ruthenium analyses were performed using an AtomScan 16, plasma emission machine.

2.2. Syntheses

Literature procedures were followed for the synthesis of $[Ru(NH_3)_5]Cl_2$ [19], $[Ru(NH_3)_5Cl]Cl_2$ [20], $[Ru(NH_3)_5(OSO_2CF_3)](CF_3SO_3)_2$ [21], *cis*- $[Ru(NH_3)_4Cl_2]Cl$ [22], $[Cr(CO)_5CN]Et_4N$ [3], $[(OC)_5Cr(\mu-CN)Ru(NH_3)_5](CF_3SO_3)_2$ and $[(OC)_5Cr(\mu-CN)Os(NH_3)_5]$

$(CF_3SO_3)_2$ [15]. *Fac*- $[Ru(NH_3)_3Cl_3]$ was prepared either by boiling a solution of *cis*- $[Ru(NH_3)_4Cl_2]Cl$ in conc. hydrochloric acid to give an orange–brown precipitate or by decomposition [23,24] of $[(NH_3)_3Ru(\mu-Cl)_3Ru(NH_3)_3]Cl_2$ in conc. hydrochloric acid in an oxygen enriched atmosphere over several days. *Fac*- $[Ru(NH_3)_3(OH_2)_3](CF_3SO_3)_3$ was prepared according to Diamantis and Moritz [25]. *Cis*- $[Ru(NH_3)_4(OSO_2CF_3)_2](CF_3SO_3)$ was prepared from *cis*- $[Ru(NH_3)_4Cl_2]Cl$ using the same procedure and conditions [21] as given for the preparation of $[Ru(NH_3)_5(OSO_2CF_3)](CF_3SO_3)_2$. The product gave satisfactory analyses. *Anal.* Found: C, 5.7; H, 2.6; N, 8.1; Cl, <0.4. *Calc.*: C, 5.9; H, 2.0; N, 9.1%.

2.2.1. Synthesis of $[Ru(NH_3)_6](CF_3SO_3)_3$

A sample of $[Ru(NH_3)_6]Cl_2$ (1 g, 3.65 mmol) is dissolved in a minimum volume of distilled water acidified with a few drops of aqueous 2 M trifluoromethanesulfonic acid to form a clear yellow solution. A few drops of aqueous hydrogen peroxide (30%) are added and following gentle warming the solution becomes colourless. After stirring the solution in an ice-bath for several minutes, white crystals are collected by filtration and washed with a little ethanol, acetone and diethyl ether. The dry white solid is placed in a two-neck round-bottom flask (25 ml) connected with a dinitrogen bubble inlet and is dissolved in neat trifluoromethanesulfonic acid (8 ml). The solution is heated (50–60 °C) for 30 min whilst a slow stream of nitrogen is passed through it. The solution is cooled and the careful addition of excess diethyl ether precipitates the product. The white powder is collected by filtration and washed with excess diethyl ether. The product can be recrystallised by dissolving this powder in a small volume of distilled water at 50 °C acidified with one drop of neat trifluoromethanesulfonic acid. Several more drops of acid are added to the clear solution which is then refrigerated (5 °C) overnight. A solid mass of white needles are isolated by filtration, washed with excess diethyl ether and vacuum dried. *Anal.* Found: C, 5.6; H, 2.9; N, 13.0. *Calc.*: C, 5.5; H, 2.8; N, 12.9%.

2.2.2. Synthesis of $[(OC)_5Cr(\mu-CN)M(NH_3)_5](PF_6)_2$ (*M* = Ru, Os (**CrRu**, **CrOs**))

These compounds are prepared quantitatively from the trifluoromethanesulfonate salts by dissolution in a tiny amount of acetone followed by the addition of water to form a clear blue (purple for *M* = Os) solution. Drops of a saturated aqueous solution of ammonium hexafluorophosphate are added to the stirred solution to yield a pale blue (dark blue for *M* = Os) precipitate. After cooling to 5 °C, the powder is collected by filtration, washed with a little ice-cold water, followed by excess diethyl ether and then vacuum dried. *Anal.* Found for *M* = Ru: C, 11.0; H, 2.2; N, 12.0. *Calc.*: C, 10.4; H, 2.2; N, 12.1%. Metal mole ratio (CF_3SO_3 salt) Cr/Ru = 1.05 (1.0). *Anal.* Found for *M* = Os: C, 9.4; H, 2.0; N, 10.4. *Calc.*: C, 9.2; H, 1.9; N, 10.7%.

The syntheses of the following cyanide-bridged compounds were carried out in the dark; solutions were subsequently manipulated in subdued light using aluminium foil.

2.2.3. Synthesis of *cis*-[$\{(OC)_5Cr(\mu-CN)\}_2Ru(NH_3)_4\}CF_3SO_3$ (**Cr₂Ru**)

Samples of *cis*-[$Ru(NH_3)_4(OSO_2CF_3)_2$] (CF_3SO_3) (0.2 g, 0.32 mmol) and [$Cr(CO)_5CN$]Et₄N (0.47 g, 0.98 mmol) are dissolved in acetone (40 ml) under nitrogen, heated (45 °C) and stirred in the dark for 3 h. The blue solution is evaporated under reduced pressure and low temperature to dryness and dissolved in methanol (60 ml). The solution was put under nitrogen again and a slurry of Sephadex CM C-25 ion exchange resin in water is added by pipette. The mixture is stirred for several minutes until adsorption of the blue solution onto the Sephadex is virtually complete. More water can be added but the ratio of water:methanol should be kept less than 1:1. The mother-liquor is decanted off and the blue coloured Sephadex is put onto the top of a column (1×6 cm) of fresh Sephadex. (The mother-liquor, if still significantly blue, can be filtered and passed through the column). The column is washed with a 1:1 water:methanol solution. The product is eluted with 0.25 M trifluoromethanesulfonic acid (1:1, methanol:water). The methanol and some of the water is removed by rotor-evaporation under reduced pressure to yield a powdery precipitate. The blue powder is separated by filtration, washed with a very small volume of dilute aqueous trifluoromethanesulfonic acid, followed by excess petroleum spirit (40–60). The solid (~0.2 g) is stirred with diethyl ether (~7 ml) and pentane (3 ml) and subsequently filtered, washed with petroleum spirit and vacuum dried. Yield: ~150 mg. *Anal.* Found: C, 20.9; H, 1.6; N, 11.1. Calc.: C, 20.7; H, 1.6; N, 11.0%. Metal mole ratio Cr/Ru = 2.1(2.0).

2.2.4. Synthesis of *fac*-[$\{(OC)_5Cr(\mu-CN)\}_3Ru(NH_3)_3\}$ (**Cr₃Ru**)

Samples of *fac*-[$Ru(NH_3)_3(OH_2)_3$] (CF_3SO_3)₃ (0.15 g, 0.23 mmol) and [$Cr(CO)_5CN$]Et₄N (0.43 g, 0.89 mmol) are dissolved in acetone (35 ml) under nitrogen and heated (45 °C) for 3 h. The blue solution is evaporated to dryness under reduced pressure and low temperature and dissolved in dichloromethane (50 ml). The green–pale blue solution is adsorbed onto a column of TLC grade silica (2–25 μm) (2×7 cm) which is then washed with excess dichloromethane and 10% tetrahydrofuran/dichloromethane to remove the pale yellow band of excess [$Cr(CO)_5CN$][−]. The blue product is best eluted as a tight band with dimethoxyethane. The blue solution is evaporated to dryness under reduced pressure and low temperature. The product is isolated by swirling with some dichloromethane, filtered, washed with petroleum spirit and vacuum dried. (If the solid dissolves it can be reprecipitated with the slow addition of hexane or petroleum spirit (40–60)). Yield: 150 mg. *Anal.* Found: C, 27.0; H, 1.25; N, 10.2. Calc.: C, 26.8; H, 1.15; N, 10.4%. Metal mole ratio Cr/Ru = 3.1(3.0).

3. Results and discussion

3.1. Syntheses

The novel trimetallic and tetrametallic complexes, **Cr₂Ru** and **Cr₃Ru**, are synthesised directly using a modest excess of the pentacarbonylcyanochromate ion and the appropriate ammineruthenium moiety. For **Cr₂Ru** the labile *cis*-bis(trifluoromethanesulfonate) (triflate) is used in an analogous fashion to the reported preparation of **CrRu**, whereas **Cr₃Ru** is synthesised using the aquo complex, *fac*-[$Ru(NH_3)_3(OH_2)_3$]³⁺. One noticeable feature in these preparations is the transient pink–red colouration observed immediately after the reagents are mixed together in acetone, which is soon replaced by the intense blue colour of the products. The pink colour arises from an outer-sphere charge transfer (OSCT) from the donor to acceptor metal fragments in an ion-pair [26] since this same colouration is observed, and remains, in mixing solutions of [$Cr(CO)_5CN$][−] and [$Ru(NH_3)_6$]³⁺ in acetone. This also provides a sensitive test for the purity of the hexaammineruthenium(III). Any ammine loss, through overheating in the chloride volatilisation step (see Section 2) with trifluoromethanesulfonic acid, would subsequently produce a blue colour upon mixing with [$Cr(CO)_5CN$][−]. None was observed for our product. All the chromium–ruthenium complexes appear air stable as solids and were successfully characterised by elemental analysis, IR, Vis–NIR spectroscopies and cyclic and square-wave voltammtries.

3.2. Infrared spectra

The profile of pressed pellet IR spectra of **CrRu** and **CrOs** (triflate salts) in the carbonyl region are described and assigned elsewhere [15]. The spectra of **Cr₂Ru** and **Cr₃Ru** show similarly shaped and broad profiles, characteristic of local C_{4v} symmetry, in the carbonyl region but with $\nu(CN) = 2100$ and 2108 cm^{-1} respectively ($\nu(CN) = 2095$ and 2101 cm^{-1} for **CrRu** and $Cr(CO)_5CN$ [−], respectively). For **Cr₃Ru**, which is neutral, there is no evidence, as expected, for the triflate ion in the IR. In **CrRu** and **CrOs** there is a sharp doublet at 1037 and 1028 cm^{-1} , whereas in **Cr₂Ru** there is only a singlet at 1027 cm^{-1} . Miles et al. [27] report Raman and IR spectra for Group I metal triflate salts and assign this band to the symmetric stretch $\nu_s(SO_3)$ assuming C_{3v} symmetry. The implication is that in **CrRu** the triflate anions are not equivalent. This is confirmed in the crystal structure, which will be reported [28] elsewhere with detailed resonance Raman results for **CrRu**, **CrOs** and the rhodium analogue, **CrRh**, (at several wavelengths) with associated analyses in respect of the MMCT excited-state geometry.

3.3. Electrochemistry

Cyclic voltammograms for **CrRu**, **Cr₂Ru** and **Cr₃Ru** recorded routinely at 100, 200, 300, 400 and 500 mV s^{−1} are

shown in Figs. 1–3, respectively. In all cases the lower potential couple ($\sim +0.05$ V versus SCE) corresponds to the ammineruthenium(III/II) process and the upper potential couple ($\sim +0.9$ V versus SCE) to the carbonylchromium(0/I) redox. No differences were observed in reversing the direction of the potential scan. The chromium and ruthenium centres in all three complexes exhibit properties associated with reversible and diffusion controlled electron transfer (peak currents, i_p , proportional to the square root of the scan rate, ν , and oxidative-to-reductive peak current ratios, $i_{p,a}/i_{p,c}=1$) to a scan rate of 20 mV s^{-1} . Accurate potentials relative to the internal standard ferrocene/ferrocenium (Fc/Fc^+) couple are detailed in Table 1. Fig. 1 also shows an extended range voltammogram for **CrRu** at 100 mV s^{-1} . The completely irreversible couple ($+1.45$ V versus SCE) which we assign to a second chromium centred oxidation, Cr(I/II) , appears to result in product decomposition as evidenced by the smaller reductive current of the Cr(0/I) couple and the extra wave at (~ 0.35 V versus SCE) which are seen in the reverse scan. For these reasons all subsequent voltammograms were restricted in range to an upper limit of $\sim +1.15$ V (versus SCE). Peak current potential separations, ($\Delta E_p = E_{p,a} - E_{p,c}$) for all the ruthenium centres are 65 ± 5 mV (at 100 mV s^{-1}), the same as for ferrocene; they increase slightly with scan rate. The ΔE_p values associated with the chromium centres similarly change little with scan rate, but vary significantly within the **Cr_xRu** set. For **CrRu**, $\Delta E_p = 65$ mV, whereas **Cr₂Ru**, $\Delta E_p = 95$ mV, exhibits an apparent dispersion and broadening within the redox wave peaks which is particularly pronounced in **Cr₃Ru** with $\Delta E_p = 135$ mV (Fig. 3). The implication is that in **Cr₂Ru** and **Cr₃Ru** the oxidation of the second (and third) chromium centres are at slightly different potentials to the first.

Square-wave voltammograms [18] for **CrRu**, **Cr₂Ru** and **Cr₃Ru** are shown in Figs. 4–6. The forward and reverse currents are shown as dotted lines and their difference as the bell-shaped solid line. The couples are referenced to that of ferrocene. Standard conditions were used, $E_{\text{sw}} = 50$ mV, $E_{\text{st}} = 5, 10$ mV at 25 Hz. The redox potentials of the metal centres (the potentials at difference current peaks) were found to be within 5 mV of those calculated from the cyclic voltammograms, $E_{1/2} = 1/2(E_{p,a} + E_{p,c})$. According to documented [29] Nernstian analysis of square-wave voltammograms for large planar electrodes, the full width ($W_{1/2}$) of the bell-shaped difference current peaks at half their height is given by Eq. (1), where n , F , R and T have their usual meanings, E_{sw} is in volts and $\zeta_{\text{sw}} = nFE_{\text{sw}}/RT$.

$$W_{1/2} = (RT/nF) \{3.53 + 3.46\zeta_{\text{sw}}^2(\zeta_{\text{sw}} + 8.1)^{-1}\} \quad (1)$$

The measured values of $W_{1/2}$ (Table 1) for **CrRu** are 124 ± 4 mV for both metal centres and ferrocene, consistent with the prediction from Eq. (1) of 123 mV at 293 K for $n=1$. The same equation predicts $W_{1/2} = 101$ and 103 mV for $n=2$ and 3, respectively, whereas Table 1 clearly shows that whilst the bandwidth of the ruthenium centres (and ferrocene) remain close to 124 mV, those of the chromium

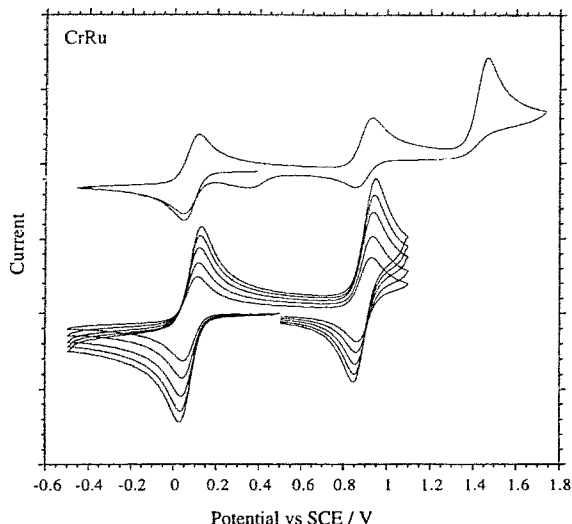


Fig. 1. Cyclic voltammograms for **CrRu** (MeCN) at 100, 200, 300, 400, 500 mV s^{-1} and extended range scan 100 mV s^{-1} .

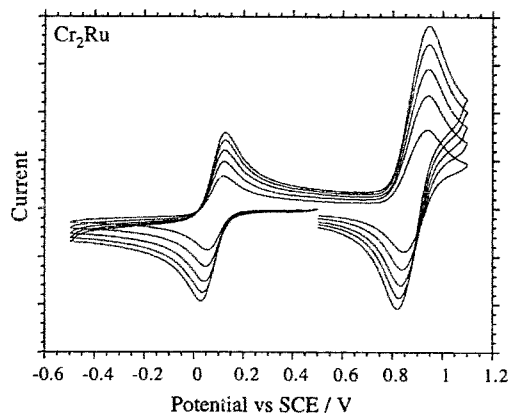


Fig. 2. Cyclic voltammograms for **Cr₂Ru** (MeCN) at 100, 200, 300, 400, 500 mV s^{-1} .

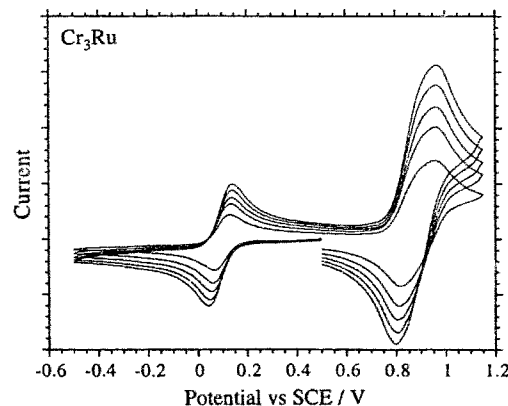


Fig. 3. Cyclic voltammograms for **Cr₃Ru** (MeCN) at 100, 200, 300, 400, 500 mV s^{-1} .

Table 1
Characteristic electrochemical data for CrRu, Cr₂Ru and Cr₃Ru^{a,b}

	CrRu		Cr ₂ Ru		Cr ₃ Ru	
ΔE_p /mV ^c	65	65	95	65	135	65
$E_{1/2}$ /V ^d	+0.45	-0.37	-0.45	-0.36	+0.445	-0.335
$W_{1/2}$ /mV ^e	125	125	155	125	200	125
Areas (SWV)	1:1		2:1		3:1	

^a Solutions of 0.1M Bu₄NBF₄ (MeCN).

^b Values for CrOs are $E_{1/2} = +0.395, -1.115$ V (vs. Fc; ± 5 mV); $\Delta E_p = 65, 65; \pm 5$ mV.

^c $\Delta E_p = E_{p,a} - E_{p,c}$ (for CVs; ± 5 mV); $E_{1/2}$ (vs. Fc; ± 5 mV) = $1/2(E_{p,a} + E_{p,c})$ (for CVs).

^d $E_{1/2}$ (vs. Fc; ± 5 mV) measured at peak current in SWV.

^e $W_{1/2}$ = SWV bandwidth (± 4 mV) at half maximum height.

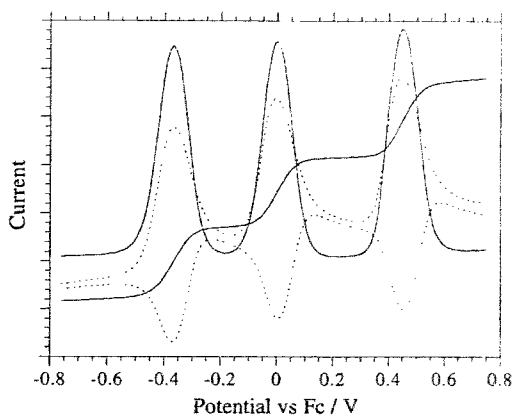


Fig. 4. Square-wave voltammogram for CrRu (MeCN). Forward and reverse currents (dotted traces), difference current and peak integrations (solid traces).

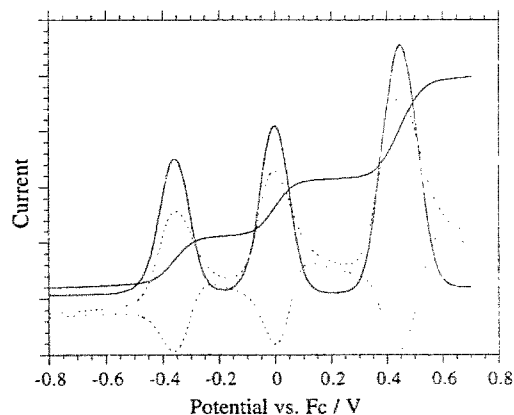


Fig. 5. Square-wave voltammogram for Cr₂Ru (MeCN). Forward and reverse currents (dotted traces), difference current and peak integrations (solid traces).

centres are much larger at 153 and 198 mV for Cr₂Ru and Cr₃Ru, respectively. This is consistent with the dispersion observed in the cyclic voltammograms indicating that the net two- and three-electron oxidations actually consist of two or three potentially distinct one-electron oxidations. To test this postulate two and three single electron SWV difference peaks

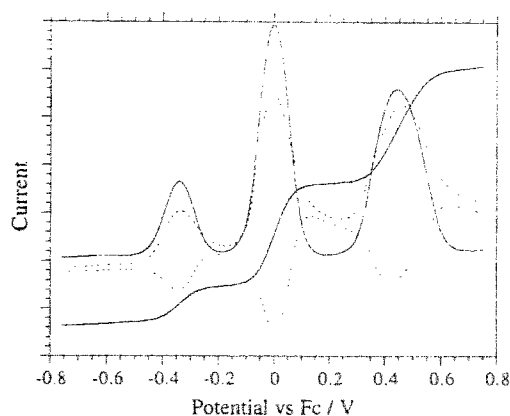


Fig. 6. Square-wave voltammogram for Cr₃Ru (MeCN). Forward and reverse currents (dotted traces), difference current and peak integrations (solid traces).

($W_{1/2} = 124$ mV) were combined computationally. The resultant modelled peaks for the chromium centres were found to mimic the observed bandwidths and the chromium:ruthenium relative peak heights for Cr₂Ru and Cr₃Ru with one-electron SWV peak separations of ~ 65 mV. The implication is that although the chromium centres are equivalent by symmetry the individual chromium centres are coupled to one another, albeit only to a small extent, through the ruthenium centre and can communicate. (A separation of 65 mV corresponds to a comproportionation constant of 13.) Taking the analysis further, as all the chromium centres are reversible, the total area (S_T) of the square-wave peaks for the chromium centres should be additive (Eq. (2)) and the integrated areas should correspond to simple multiples. The ruthenium centre in each case provides an internal standard in that it defines the area expected for a one-electron reversible couple at the same concentration (c^*) and under the same conditions. (In Eq. (2), A is the planar electrode surface area, f , the square-wave frequency and D the diffusion coefficient.)

$$S_T = 1.931nFc^*AE_{SWV}(Df)^{1/2} \quad (2)$$

Figs. 4–6 show the sigmoidal shaped integrations for the difference current peaks and confirm the expected ratios of

1:1, 2:1 and 3:1 (within 5%) for **CrRu**, **Cr₂Ru** and **Cr₃Ru**, respectively in agreement with the analytical Cr/Ru mole ratio results.

Another feature characteristic of the **Cr_xRu** set is the virtually invariant redox potentials of both the polyamine-ruthenium and pentacarbonylchromium centres. Previous comments [15] that $[(OC)_5Cr-CN]^-$, and other cyanide fragments, behave as pseudo ammine ligands is verified. For comparison the reduction potential for the hexaammineruthenium(III) tris(trifluoromethanesulfonate) under the same conditions is -0.37 V (versus Fc).

3.4. Electronic absorption

Absorption spectra were recorded within 5 min of sample dissolution (~ 3 mg/10 ml) as the absorbance of some solutions appeared to decrease within 1 h especially in the air and sunlight. The most unstable in this respect was **Cr₃Ru** in hexamethylphosphoramide.

Organic solutions of **CrRu**, **Cr₂Ru**, **Cr₃Ru** and **CrOs** are intensely coloured in the visible region (Figs. 7–10). The absorptions are assigned to MMCT transitions from the chromium (d^6) centre to the Group VIII ammine metal (d^5) centre through the cyanide bridge. The corresponding characteristic parameters, energy, bandwidth and intensity are shown in Tables 2 and 3. They are typical for such Robin-Day Class II systems [16].

The spectra are clearly solvatochromic. The solution colours for the **Cr_xRu** set vary from pale blue–green to deep blue or purple whereas for the **CrOs** system the diversity of visible colours is quite spectacular. In nitromethane (NM) it is royal blue, acetonitrile (AN) blue–purple, acetone (ACET) red–purple, trimethylphosphate (TMP) red–pink, dimethylformamide (DMF) orange and hexamethylphosphoramide (HMPA) yellow. Ammine complexes of ruthenium(II/III), and presumably osmium(II/III), are known to exhibit solvatochromic [16,30] MLCT, LMCT and MMCT transitions originating from the preferential stabilisation of the ruthenium(III) state to the ruthenium(II) state through outer-sphere hydrogen bonding between Lewis donor sol-

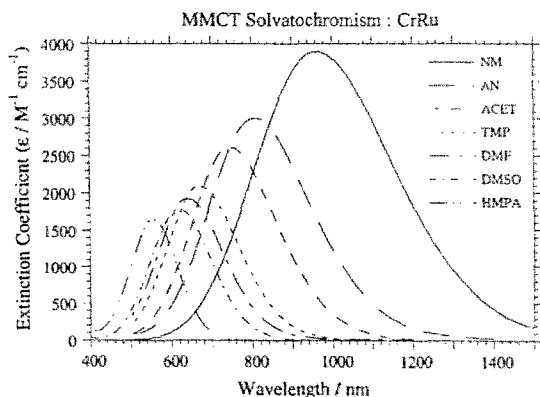


Fig. 7. Solvatochromism of the MMCT band for **CrRu**.

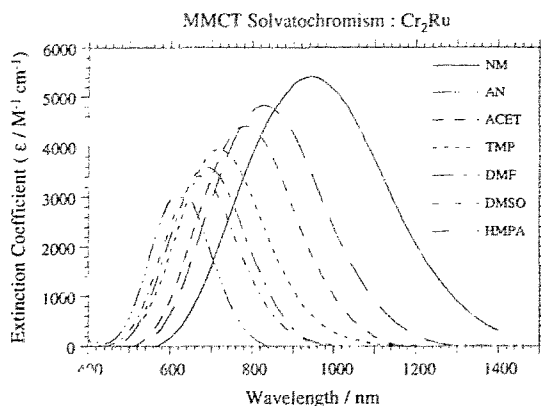


Fig. 8. Solvatochromism of the MMCT band for **Cr₂Ru**.

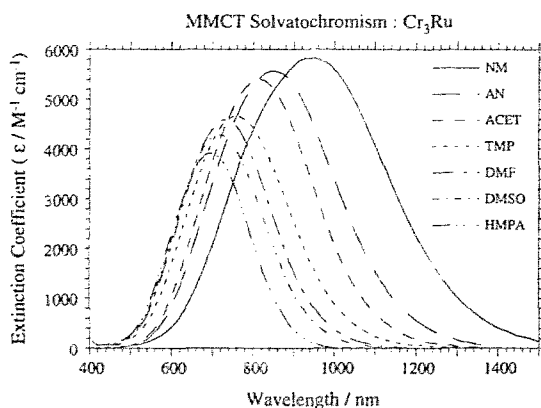


Fig. 9. Solvatochromism of the MMCT band for **Cr₃Ru**.

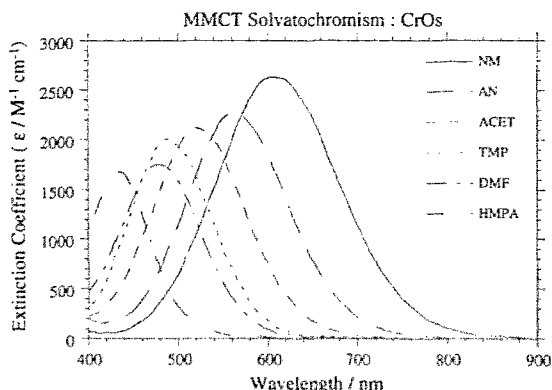


Fig. 10. Solvatochromism of the MMCT band for **CrOs**.

vents and the acidic ammine protons. Effects have been correlated adequately using the Gutmann solvent donor number (DN) scale [31,32]. The profiles (Figs. 7–10) all show the expected increase in CT energy with solvent donicity together with a decreasing intensity on account of increased electronic potential asymmetry between the ground and excited states and thus reduced coupling [16].

The total shift in MMCT energy from nitromethane to hexamethylphosphoramide is greatest for **CrRu** (~ 7700

Table 2
MMCT band characteristics for **CrRu**, **Cr₂Ru** and **Cr₃Ru** in various aprotic organic solvents

Solvent ^a	CrRu			Cr₂Ru			Cr₃Ru		
	ν_{max} (cm ⁻¹) (nm)	ϵ_{max} (M ⁻¹ cm ⁻¹)	$\Delta\nu_{1/2}$ (cm ⁻¹)	ν_{max} (cm ⁻¹) (nm)	ϵ_{max} (M ⁻¹ cm ⁻¹)	$\Delta\nu_{1/2}$ (cm ⁻¹)	ν_{max} (cm ⁻¹) (nm)	ϵ_{max} (M ⁻¹ cm ⁻¹)	$\Delta\nu_{1/2}$ (cm ⁻¹)
Nitromethane (NM) (2.7) ^b	11010 (908)	3640	4450	10580 (945)	5410	4840	10525 (950)	5850	5010
Nitromethane (NM) (2.7) ^c	10305 (970)	3900	4340						
Chloroacetonitrile (CIAN)	10695 (935)	3570	4500						
Acetonitrile (AN) (14.1)	12345 (810)	3605	4500	12045 (830)	4830	4700	11785 (882)	5570	5010
Acetone (ACET) (17.0)	13330 (750)	2610	5160	12770 (783)	4410	4640	12220 (818)	5410	4850
Trimethylphosphate (TMP) (23.0)	14835 (674)	2090	4670	13935 (718)	3945	4840	13155 (707)	4650	4975
Dimethylformamide (DMF) (26.6)	15575 (642)	1930	4690	14510 (689)	3590	4660	13620 (732)	4585	4885
Dimethyl sulfoxide (DMSO) (29.8)	16100 (621)	1780	4570	14880 (671)	3410	4740	13885 (719)	4285	4930
Hexamethylphosphoramide (HMPA) (38.8)	18015 (555)	1650	4490	16050 (623)	3135	4570	14450 (692)	3920	4750

^a Numbers in parentheses refer to Gutmann solvent donor numbers.

^b Data for **CrRu** triflate salt.

^c Data for **CrRu** hexafluorophosphate salt.

Table 3
MMCT band characteristics for **CrOs** in various aprotic organic solvents

Solvent ^a	CrOs		
	ν_{max} (cm ⁻¹) (nm)	ϵ_{max} (M ⁻¹ cm ⁻¹)	$\Delta\nu_{1/2}$ (cm ⁻¹)
Nitromethane (NM) (2.7) ^b	16690 (599)	2540	4520
Nitromethane (NM) (2.7) ^c	16260 (615)	2635	4490
Acetonitrile (AN) (14.1)	18980 (553)	2260	4570
Acetone (ACET) (17.0)	19080 (524)	2120	4500
Trimethylphosphate (TMP) (23.0)	20200 (495)	2010	4495
Dimethylformamide (DMF) (26.6)	20745 (482)	1750	4710
Hexamethylphosphoramide (HMPA) (38.8)	22930 (436)	1680	4960

^a Numbers in parentheses refer to Gutmann solvent donor numbers.

^b Data for triflate salt.

^c Data for hexafluorophosphate salt.

cm⁻¹), smallest for **Cr₃Ru** (~3800 cm⁻¹) with **Cr₂Ru** in between at ~5500 cm⁻¹. Linear regression analyses of the MMCT energy as a function of solvent donicity are shown in Fig. 11 and quantitatively indicate the CT sensitivity to the outer-sphere environment. Simplistically, one would expect this sensitivity, reflected in the gradients, to be directly proportional to the number of solvent molecules in the immediate second sphere or conversely to the number of ammine ligands sterically accessible to participate in outer-sphere hydrogen bonding. Although there are only three data points, 219(±7), 158(±7) and 116(±8) cm⁻¹/DN for **CrRu**, **Cr₂Ru** and **Cr₃Ru**, respectively, the resulting linear correlation is ~51(±6)cm⁻¹/DN/ammine group (*R* = 0.994)

which should be compared to the limited electrochemical data given by Hupp and Weaver [33] (~37.9 cm⁻¹/DN/ammine) and spectroscopic data by Meyer and co-workers [30] for the complex set, [Ru(NH₃)₂(bipyridine)₂]²⁺ (*λ* = 1–3). In the limit of weak outer-sphere effects (e.g. in nitromethane) the sensitivity correlations converge to a point confirming the approximate ligating equivalence of NH₃ and Cr(CO)₃CN⁻ in these systems. The solvent sensitivity of **CrOs**, 188(±7) cm⁻¹/DN, (total shift ~6700 cm⁻¹) is slightly smaller than that of the ruthenium analogue probably on account of the former's larger size, its smaller positive charge density and subsequent weaker ammine acidity. The large solvent shifts for **CrRu** (7700 cm⁻¹) and **CrOs** (6700

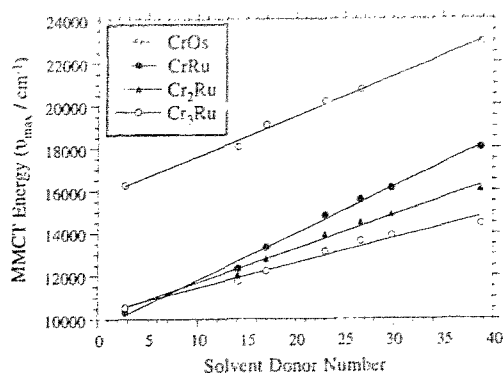


Fig. 11 Linear regression correlations for solvent dependent MMCT energies for CrOs, CrRu, Cr₂Ru and Cr₃Ru. CrOs: ν_{\max} (cm^{-1}) = 15720(160) + 188(7)DN; $R=0.997$. CrRu: ν_{\max} (cm^{-1}) = 9610(170) + 219(7)DN; $R=0.997$. Cr₂Ru: ν_{\max} (cm^{-1}) = 10110(170) + 158(7)DN; $R=0.995$. Cr₃Ru: ν_{\max} (cm^{-1}) = 10280(200) + 116(8)DN; $R=0.988$.

cm^{-1}) are worth comparing with the hypsochromic intramolecular CT transition of pyridinium *N*-phenol betaine. It forms the basis of the well-known and most comprehensive E_T solvent scale. Reichardt reports [34] a shift of $\sim 9700 \text{ cm}^{-1}$ for this betaine from 453 nm (water) to 810 nm (diphenylether).

One of the reasons for converting the triflate salt of CrRu into the hexafluorophosphate salt was to enhance its solubility in the weakly donating solvents, nitromethane and chloroacetonitrile. Surprisingly it was found that the MMCT energy seemed to depend significantly on the counter ion. Tables 2 and 3 show that for this anion exchange there is a difference of up to 700 cm^{-1} in nitromethane even though the chromophore concentration is only around 0.2 millimolar. In acetonitrile and higher donating solvents this anion exchange produced little or no change in the CT energy, however, this single point energy change alters the gradient for CrRu (Fig. 11) from 200 to $219 \text{ cm}^{-1}/\text{DN}$. Similar effects occur for CrOs; the triflate salt is purple but the hexafluorophosphate salt is royal blue. Such anion outer-sphere sensitivity is worth further investigation in respect of chemical sensing using optical and electrochemical probes.

Table 2 and Figs. 7–9 also show that the intensity and bandwidth, and therefore the integrated intensity for the Cr_{*n*}Ru series increases with the number of chromium groups. One intuitively expects this on account of the greater transition probability for the MMCT with increasing the number of bound chromium centres but analysis reveals that there appears to be no simple correlation for this observation.

With the recent reported [35] synthetic methods into *cis*-tetraammine- and *fac*-triammine-osmium chemistry, the analogues, Cr₂Os and Cr₃Os should be accessible.

Acknowledgements

We thank Dr F.A. Armstrong for the use of electrochemical facilities and the S.E.R.C. for post-doctoral support (W.M.L.).

References

- [1] Y. Dong and J.T. Hupp, *Inorg. Chem.*, **31** (1992) 3170.
- [2] W.M. Laidlaw and R.G. Denning, *Inorg. Chim. Acta.*, **219** (1994) 121.
- [3] W.M. Laidlaw and R.G. Denning, *Polyhedron*, **13** (1994) 1875.
- [4] M.B. Robin and P. Day, *Adv. Inorg. Chem. Radiochem.*, **10** (1967), 247.
- [5] C.A. Bignozzi, S. Roffia and F. Scandola, *J. Am. Chem. Soc.*, **107** (1985) 1644.
- [6] C.A. Bignozzi, C. Paradisi, S. Roffia and F. Scandola, *J. Am. Chem. Soc.*, **27** (1988) 408.
- [7] C.A. Bignozzi, C. Chiorboli, M.T. Indelli, F. Scandola, V. Bertolasi and G. Gilli, *J. Chem. Soc., Dalton Trans.*, (1994) 2391.
- [8] M.A. Watzky, X. Song and J.F. Endicott, *Inorg. Chim. Acta*, **226** (1994) 109.
- [9] P. Braunstein, D. Cauzzi, D. Kelly, M. Lanfranchi and A. Tiripicchio, *Inorg. Chem.*, **32** (1993) 3373.
- [10] H. Kunkely, V. Pawlowski and A. Vogler, *Inorg. Chim. Acta*, **225** (1994) 327.
- [11] H. Kunkely and A. Vogler, *Inorg. Chim. Acta*, **209** (1993) 93.
- [12] Y. Wu, C. Cochran and A.B. Bocarsly, *Inorg. Chim. Acta*, **226** (1994) 251.
- [13] B.W. Pfenning and A.B. Bocarsly, *Coord. Chem. Rev.*, **111** (1991) 91.
- [14] C.A. Bignozzi, R. Argazzi, C. Chiorboli, S. Roffia and F. Scandola, *Coord. Chem. Rev.*, **111** (1991) 261.
- [15] W.M. Laidlaw and R.G. Denning, *Polyhedron*, **13** (1994) 2337.
- [16] W.M. Laidlaw and R.G. Denning, *J. Chem. Soc., Dalton Trans.*, (1994) 1987.
- [17] W.M. Laidlaw, *D. Phil. Thesis*, University of Oxford, 1993.
- [18] J. Osteryoung and J.J. Odea, in A.J. Bard (ed.), *Electroanalytical Chemistry*, Vol. 14, Marcel Dekker, New York, 1986, p.209.
- [19] J.E. Fergusson and J.L. Love, *Inorg. Synth.*, **13** (1972) 208.
- [20] J.P. Chang, E.Y. Fung and J.C. Curtis, *Inorg. Chem.*, **25** (1986) 4233.
- [21] G.A. Lawrence, P.A. Lay, A.M. Sargeson and H. Taube, *Inorg. Synth.*, **24** (1986) 257.
- [22] S.D. Pell, M.M. Sherhan, V. Tramontano and M.J. Clarke, *Inorg. Synth.*, **26** (1989) 65.
- [23] E.E. Mercer and L.W. Gray, *J. Am. Chem. Soc.*, **94** (1972) 6426.
- [24] F. Botti and S.B. Tong, *Can. J. Chem.*, **49** (1971) 3739.
- [25] A.A. Diamantis and P.S. Moritz, *Aust. J. Chem.*, **46** (1993) 221.
- [26] A. Vogler and J. Kisslinger, *J. Am. Chem. Soc.*, **104** (1982) 2311.
- [27] M.G. Miles, G. Doyle, R.P. Cooney and R.S. Tobias, *Spectrochim. Acta, Part A*, **25** (1969) 1515.
- [28] J.L. Wootton, W.M. Laidlaw, J.I. Zink and R.G. Denning, unpublished results.
- [29] K. Aoki, K. Maeda and J. Osteryoung, *J. Electroanal. Chem.*, **272** (1989) 17.
- [30] J.C. Curtis, B.P. Sullivan and T.J. Meyer, *Inorg. Chem.*, **22** (1983) 224.
- [31] Y. Marcus, *Chem. Soc. Rev.*, **22** (1993) 409.
- [32] V. Gutmann, *Electrochim. Acta*, **21** (1976) 661.
- [33] J.T. Hupp and M.J. Weaver, *J. Phys. Chem.*, **89** (1985) 1601.
- [34] C. Reichardt, *Angew. Chem., Int. Ed. Engl.*, **4** (1965) 29.
- [35] Z.W. Li, W.D. Harman, P.A. Lay and H. Taube, *Inorg. Chem.*, **33** (1994) 3635.